Braz J Phys (2013) 43:145–151
DOI 10.1007/s13538-013-0125-2

SOCIEDADE BRASILEIRA DE FÍSICA

GENERAL AND APPLIED PHYSICS

Breakdown Voltage Distributions in Ne-Filled Diode at 1.33 mbar with Corona Appearance in Pre-breakdown Regime

Miodrag K. Radović · Čedomir A. Maluckov · Jugoslav P. Karamarković · Saša A. Rančev · Slobodan D. Mitić

Received: 10 February 2012 / Published online: 3 April 2013

Abstract The electrical breakdown of a gas subject to an up-ramping external voltage is studied, experimentally and theoretically, under conditions leading to the appearance of a positive corona at the anode in the pre-breakdown regime. Experimentally, voltage ramps with various rates k in the interval ranging from 0.3 V/s to 26 kV/s are applied to the diode, with the histogram of breakdown voltages being recorded for each rate. The theoretical model gives attention to the pre-breakdown multiplication causing the corona, which tends to reduce the statistical time delay t_S before the primary electron is released and hence to make t_S comparable to the formative time t_F. The multiplication being therefore expected to affect the voltage dependence of the electron yield, a nonlinear equation relating the yield to the overvoltage is introduced. The resulting theoretical expression for the breakdown voltage distribution agrees well with the experimental histograms. Especially noteworthy is the good agreement with the low-voltage tail of the distribution, a segment of the data that has challenged previous theoretical analyses of the problem.

Keywords Electrical breakdown · Breakdown voltage distribution · Corona discharge.

1 Introduction

The electrical breakdown of a gas amounts to a transition from the dielectric to the conducting state. The transition occurs at a breakdown voltage U_B that must be treated statistically, so numerous are the microscopic variables upon which it depends [1]. Besides subsidizing practical applications, the research on electrical breakdown in gases has provided much information on the microscopic processes occurring in and on the characteristics of gaseous substances [2–4]. Given its statistical nature, the breakdown can be treated macroscopically as a stochastic phenomenon. Early work along this line of research is due to Zuber and von Laue [5, 6]. The statistical theory of electrical breakdown was later developed by Loeb [7] and Wijsman [8] in the late 1940s. The theory builds upon the mechanism first discussed by Townsend [9], who considered pressures and overvoltages sufficiently small to make space-charge effects negligible. Under such conditions, free electrons are chiefly produced by multiplications induced by the electric field. The multiplication comprises two stages: a primary ionization, characterized by a coefficient α, and multiple secondary ionizations, collectively characterized by a coefficient γ. With the limiting factors that restrict the growth

M. K. Radović
Department of Physics, Faculty of Science and Mathematics, University of Niš, Niš, Serbia

Č. A. Maluckov (✉)
Technical Faculty in Bor, University of Belgrade, Vojske Jugoslavije 12, 19210 Bor, Serbia
e-mail: cmaluckov@tf.bor.ac.rs

J. P. Karamarković
Faculty of Civil Engineering and Architecture, University of Niš, Niš, Serbia

S. A. Rančev
Faculty of Science and Mathematics, University of Nis, Nis, Serbia

S. D. Mitić
Max Planck Institute for Extraterrestrial Physics, Garching, Germany

of the electrical current in real circuits being disregarded, the following equation defines the Townsend criterion for breakdown:

$$\gamma\left(e^{\int_0^d \alpha\, \mathrm{d}x} - 1\right) = 1, \tag{1}$$

where d is the gap width.

In Eq. (1), the exponential on the left-hand side is the number of ions created by an electron, while the entire left-hand side represents the number of electrons released from the cathode by the ions. The equality therefore implies that each electron flowing from the cathode to the anode is replaced by at least one new electron at the cathode. The lowest applied voltage satisfying the criterion is called the static breakdown voltage, denoted U_S.

Given the statistical nature of ion creation and electron multiplication, no specific breakdown voltage can be predicted. Instead, a breakdown probability $P(U)$ is associated with each voltage U exceeding U_S. Towsend's theory, in which breakdown processes initiated by distinct electrons are independent, leads to the following expression relating the probability to the gap width d [1]:

$$P(U) = 1 - \frac{1}{\gamma(e^{\alpha d} - 1)}, \tag{2}$$

which is valid under the assumption that the secondary electrons start an electronic avalanche.

Two characteristic times are involved in the breakdown. The first is the time delay t_S necessary to free an initial electron, a statistical variable with exponential distribution [1]. The second interval, defined by the dynamics of impact ionization and carrier multiplication in the gas, is the formative time delay t_F, which follows a Gaussian distribution [10, 11]. The total breakdown time delay is the sum $t_D = t_S + t_F$ [1].

When a steadily growing voltage is applied to the diode, the formative period can be divided into three stages [12]. The first stage begins with the appearance of the initial electron and ends when the threshold voltage is reached. The second stage is defined by the avalanche, which creates a conduction channel between the anode and cathode. In the final stage, a significant reduction in the discharge voltage is observed as a result of conduction in the plasma channel [12].

Pre-breakdown electron multiplication has also been observed. Pre-breakdown light emission near the anode was reported in Wagenaars [13], which attributed the luminosity to early discharge. Radović et al. [14] found the pre-breakdown light emission to be affected by corona discharge on the rod-shaped anode.

If the applied voltage U ramps up at a rate $k = dU/dt$, the breakdown condition (1) is satisfied when the voltage reaches the static breakdown voltage U_S. Like the processes upon which it depends, the breakdown has a statistical nature and is characterized by a distribution $f(U_B)$. The problem of deriving this function from realistic theoretical models has fueled research in the last decades.

The first models neglected the formative time and only considered the influence of the statistical time delay upon the breakdown [15, 16]. Subsequent work gave attention to the formative time delay [15, 17–21]. In these more recent models, the applied voltage reaches an initial value U_F at the end of the constant formative time interval. Although the resulting shifted distributions $f(U_B)$ proved to be more accurate than the results reported in Radović et al. [15] and Pejović and Filipović [16], the agreement with experimental data at small voltages, i. e., in the left-hand tail of the distribution, is poor. The disagreement is a direct consequence of introducing a constant to represent the formative time, instead of a Gaussian distribution. The aforementioned disagreement may be difficult to discern in the exponential scale of Laue diagrams.

Here, we want to obtain experimental and theoretical results for the breakdown voltage distribution in a diode marked by a positive corona at the anode in the pre-breakdown regime. When the voltage rises with time in a gas diode, the corona is only a segment in the breakdown process. The multiplication that originates the corona is nonetheless important, because it raises the yield Y, i. e., the number of free electrons produced near the cathode per second. Our estimation of the breakdown voltage distribution is based on the assumption that the yield rises nonlinearly with the voltage applied to the diode gap.

2 Electrical Breakdown Density Distribution

The model here proposed to describe the breakdown voltage distribution is more realistic than the one in Radović and Maluckov [20, 21] because it allows for nonlinear voltage dependence of the yield. Otherwise, our derivation of the probability distribution is similar to previous approaches based on Townsend's breakdown mechanism.

The voltage across the gap grows linearly with time at the rate k until it reaches the breakdown voltage U_B. Let $\mathbf{U}$ be a discrete random variable with values U. To specify that the breakdown cannot occur until the voltage becomes equal to U_B, we write $\{\mathbf{U} > U_B\}$. With this notation, under the condition $\{\mathbf{U} > U_B\}$, we can determine the function $F_{\mathbf{U}|\mathbf{U}>U_B}(U)$, which defines the distribution of the random variable $\mathbf{U}$. Let $P(\mathbf{U} > U_B)$ denote the probability of breakdown for a voltage $\mathbf{U}$ greater than U_B, and $P(\mathbf{U} < U, \mathbf{U} >$

U_B) denote the probability of breakdown for a voltage $\mathbf{U}$ in the interval (U, U_B). Then we have that

$$F_{\mathbf{U}|\mathbf{U}>U_B}(U) = \begin{cases} \dfrac{P(\mathbf{U} < U, \mathbf{U} > U_B)}{P(\mathbf{U} > U_B)} = \dfrac{F(U) - F(U_B)}{1 - F(U_B)} & (U > U_B) \\ 0 & (U < U_B) \end{cases}. \tag{3}$$

With the definition $f_{\mathbf{U}|\mathbf{U}>U_B}(U) \equiv dF_{\mathbf{U}|\mathbf{U}>U_B}(U)/dU$, the following result is obtained for $U = U_{B+}$, where the + sign indicates a voltage infinitesimally larger than U_B:

$$f_{\mathbf{U}|\mathbf{U}>U_B}(U) = \frac{f(U)}{1 - F(U_B)} = \frac{F'(U)}{1 - F(U_B)} = \beta(U). \tag{4}$$

The last equality on the right-hand side of Eq. (4) defines the function $\beta(U)$, equal to the probability that the breakdown will occur in the interval $(U_B, U_B + \Delta U)$, given that there was no breakdown at the voltage U_B. Here, the interval ΔU is so small that only one breakdown can occur within it.

The function $\beta(U)$ gives the number of breakdowns in the interval ΔU. Since the voltage rises at the rate k, the number of breakdowns per unit time at the voltage U, i. e., the breakdown rate, is $\beta(U)k$. On the other hand, since the rate of electron emission from the cathode is the yield $Y(U)$ and since every emitted electron causes breakdown at the voltage U with probability $P(U)$, the breakdown rate at the voltage U is also equal to $Y(U)P(U)$. We therefore obtain an expression relating the breakdown probability $\beta(U)$ to the yield:

$$\beta(U) = Y(U)P(U)/k. \tag{5}$$

In the so-called dynamic experimental method, a ramp-up pulse is applied to the diode. The yield per applied Volt is then the *reduced yield* Y/k. At high rates k, the voltage distribution is shifted, so that the static breakdown voltage U_S is replaced by the initial voltage U_{IN}, as long as the latter exceeds U_S.

We now go back to last equality on the right-hand side of Eq. (4), substitute the right-hand side of Eq. (5) for $\beta(U)$ and solve the resulting differential equation to find the expression

$$F(U_B) = 1 - \exp\left(-\int_{U_S}^{U_B} \frac{P(U)Y(U)}{k}\,\mathrm{d}U\right). \tag{6}$$

Differentiation of both sides of Eq. (6) with respect to U yields the following result for the probability density of breakdown voltages:

$$f(U_B) = \frac{P(U)Y(U)}{k} \exp\left(-\int_{U_S}^{U_B} \frac{P(U)Y(U)}{k}\,\mathrm{d}U\right). \tag{7}$$

To compute the right-hand side of Eq. (7), we need an expression for the voltage-dependence of the yield. We assume that Y grows nonlinearly with the overvoltage and is given by the equality

$$Y(U) = Y_0 + A(U - U_S)^B. \tag{8}$$

The first term on the right-hand side is the yield at the moment when the applied voltage becomes equal to the static breakdown voltage, before corona ignition. Y_0 is therefore time-independent, a constant determined by the incidence of cosmic rays or the effects of other external sources. The coefficient A and the exponent B are rate-dependent constants, which must be obtained from fits to the experimental data.

The nonlinear voltage dependence of the yield is due to the pre-breakdown multiplication of the electrical carriers in the diode. Pre-breakdown multiplication has been reported to occur at least 3 ms before any current above significant current, above 1 μA, could be measured [22]. This finding has confirmed the supposition that the formative time delay is longer than registered by standard electrical instruments, such as the oscilloscope. The appearance of corona at the anode suggest that the time preceding the stationary regime is approximately 10 ms [22]. The multiplication processes are different for different ramp rates. The pre-breakdown multiplications are more pronounced for electrode geometries such that the electric field between the electrodes is nonuniform, because the inhomogeneity favors the formation of a corona discharge, which affects the breakdown [23].

The breakdown probability $P(U)$ is computed numerically, from Eq. (2). The ionization coefficient α is found by the numerical code BOLSIG (http://www.siglo-kinema.com/download.htm), with the corrections prescribed in Raizer [24] for electric field-to-pressure ratios in the 1,000–2,000 V /(cm mbar) range, which encompasses the experimental conditions. The code solves the Boltzmann equation for electrons in a weakly ionized gas subject to a uniform electric field, which is a typical experimental condition in the bulk of collisional low-temperature plasmas. The electron distribution is determined by the balance between electric acceleration and momentum and energy loss due to collisions with neutral gas particles. The electron transport coefficients and the collision-rate coefficients, computed from the collision cross section data, are output. The secondary-emission coefficient γ is obtained from the breakdown criterion (1).

3 Static Breakdown Voltage

As defined in Section 1, the static breakdown voltage is the lowest voltage satisfying the Townsend criterion (1). Since breakdown can occur, with probability $P(U)$, at any voltage

U above the static breakdown voltage U_S, the latter can only be approximately determined.

Previous measurements with voltage ramps have shown that electrical breakdown occurs only for voltages U_B larger than an initial voltage U_{IN}, which is always above U_S [15–21]. This can be understood as follows. The breakdown voltage can be written in the form $U_B = U_S + k(t_S + t_F)$. Since the formative time t_F for given rate k is nearly constant, an initial voltage $U_{IN} = U_S + kt_F$ naturally arises. A good estimate for U_{IN} is therefore the minimum breakdown voltage in a set of numerous measurements. To determine the static breakdown voltage U_S, one only has to find the limiting value of U_{IN} as the linear rate k approaches zero, i. e., use the expression

$$U_S = \lim_{k\to 0} U_{B\min}. \tag{9}$$

In practice, a sequence of experiments at various rates k is conducted, the minimal breakdown voltage at each k is recorded, and U_S is determined by fitting the set of minimal voltages to Eq. (9) [21].

4 Experimental

All measurements were carried out in a neon-filled diode with 300 cm^3 tube volume. The shapes of the electrodes are distinct. The Cu cathode is cylindrical, with 6.5 mm diameter and 6.5 mm height. The anode is simply a Mo unpolished rod with 2 mm diameter. The gap separating the front base of the cathode from the tip of the anode is 24 mm. The gas tube was constructed on the basis of the X-ray tube standard. After construction, the tube was baked at 350 °C and pumped down to 10^{-7} mbar pressure. The tube was then filled with Matheson research-grade neon at 1.33 mbar pressure.

Figure 1 shows the experimental layout. A desktop computer (PC) generates a linearly rising voltage pulse, which controls the output of a Spellman MPS10P10/24 High-Voltage Power Supply. The breakdown voltages are detected by a Tektronix TDS 2012B digital-storage oscilloscope, the results being transferred to the PC for analysis. Each experimental sequence involved 1,500 successive, independent measurements.

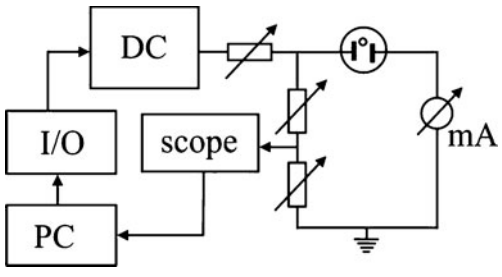

Fig. 1 Experimental Layout. *DC* is the high-voltage power supply; *I/O* represents the interface module; *scope*, the oscilloscope (Tektronix TDS 2012B); mA, a milliamperemeter; and *PC*, a desktop computer

5 Results

The mean $\bar{U}_B$ and minimal $U_{B\min}$ breakdown voltages in one of the sequences are plotted as functions of the rate k in Fig. 2, represented by the symbols • and ■, respectively. The error bars centered at the filled circles display the standard deviations. To obtain the static breakdown voltage U_S from Eq. (9), the expression $U_B = U_S + \sqrt{Gk}$, with adjustable parameters U_S and G, was fitted to the filled squares. The values $U_S = 254.4$ V and $G = 4.1$ Vs were found to optimize the fitting.

Given the good fit to the filled squares in Fig. 2, one may wonder if the filled circles likewise follow a $\sqrt{k}$ law. To discuss this question, Fig. 3 shows $\bar{U}_B - U_S$ and $\bar{U}_{B\min} - U_S$ as functions of $\sqrt{k}$. Visual inspection shows that the dashed line fits the filled circles representing $\bar{U}_{B\min} - U_S$ better than the solid line fits the open squares representing $\bar{U}_{B\min} - U_S$. This is confirmed by the correlation coefficients r next to the straight lines, since the coefficient of the dashed line comes closer to unity than the coefficient of the solid line.

5.1 Breakdown Voltage Distributions

Figure 4 shows the breakdown voltage distributions for rates k varying from 0.3 V/s to 26 kV/s. Each panel shows a histogram of 1,500 successive, independent measurements of the breakdown voltage. In each histogram, the bin width ΔU_B is chosen to accommodate roughly 20 % of the measurements in the most populated bin. To normalize the

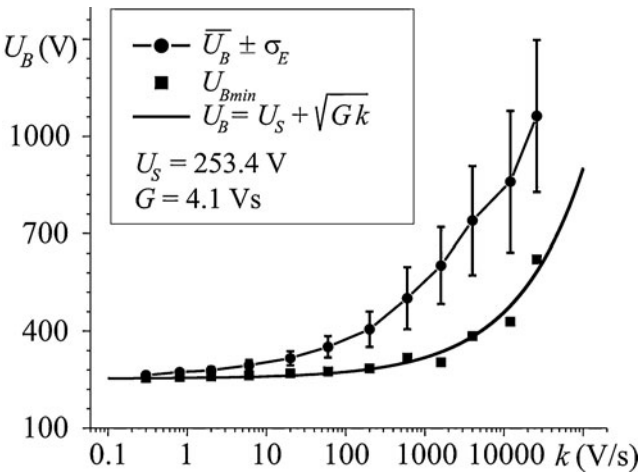

Fig. 2 Minimal ($U_{B\min}$) and mean values ($\bar{U}_B$) of the breakdown voltage as functions of the ramp-up rate k

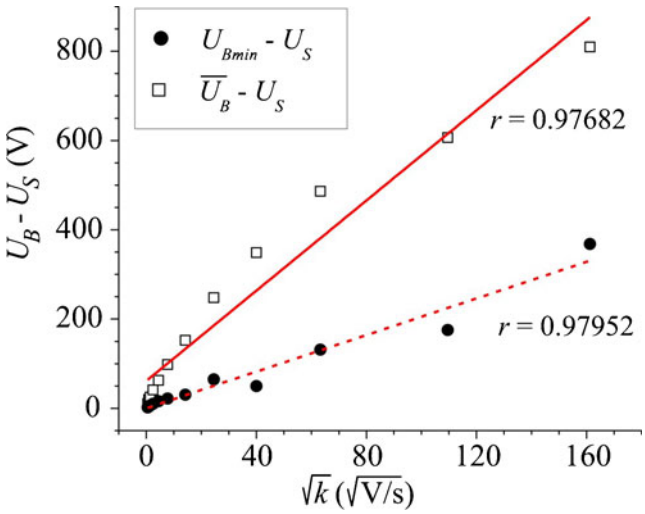

Fig. 3 (Color online) Minimal voltage $U_{B\min}$ (*filled squares*) and mean voltage $\bar{U}_B$ (*open squares*), both measured from the static breakdown voltage U_S, as functions of $\sqrt{k}$. The *dashed and solid straight lines* (*red* online) are linear regressions to the *filled squares and open squares*, respectively. In each case, the resulting correlation coefficient r is presented next to the line

histograms, the vertical scale shows the relative frequency in each interval divided by ΔU_B.

The solid lines in Fig. 4 compare the theoretical breakdown voltage distribution in Eq. (7), derived on the basis of the model proposed in Section 2, with the experimental histograms. Good agreement is found even in the rightmost panels, in which the histograms are broadest because the data were collected at the highest ks and the high- and low-voltage tails are relatively prominent.

The coefficients A and B in the nonlinear relation (8), which models the voltage dependence of the yield, are shown as functions of the rate k in Figs. 5a, b, respectively. At each rate, the data points displayed in the two panels were obtained by freely varying the two coefficients and choosing the pair that minimizes χ^2 in the comparison with the experimental distribution. The initial yield Y_0, i. e., the yield in the absence of corona, is independent of k: $Y_0 = 0.01\,/\text{s}$.

Figure 5a shows A as function of the ramp-up rate k in linear (filled squares) and logarithmic (open squares) scales. The logarithmic plot shows that A decays by nearly five orders of magnitude. The open squares are fairly well fitted by a straight line, with linear regression coefficient $r \approx -0.96$, which suggests the power law $A = a'k^b$, where $a' = 10^a$, and a and b are the coefficients shown in the box at the top-right corner of Fig. 5a. The straight line in Fig. 5b is a (somewhat inferior, with $r = 0.95$) fit to the open circles suggesting the logarithmic dependence $B = a + b\log_{10} k$, where a and b are the coefficients in the box at the top-left corner of Fig. 5b. The voltage dependence of the yield is dominantly determined by the exponent B on the right-hand

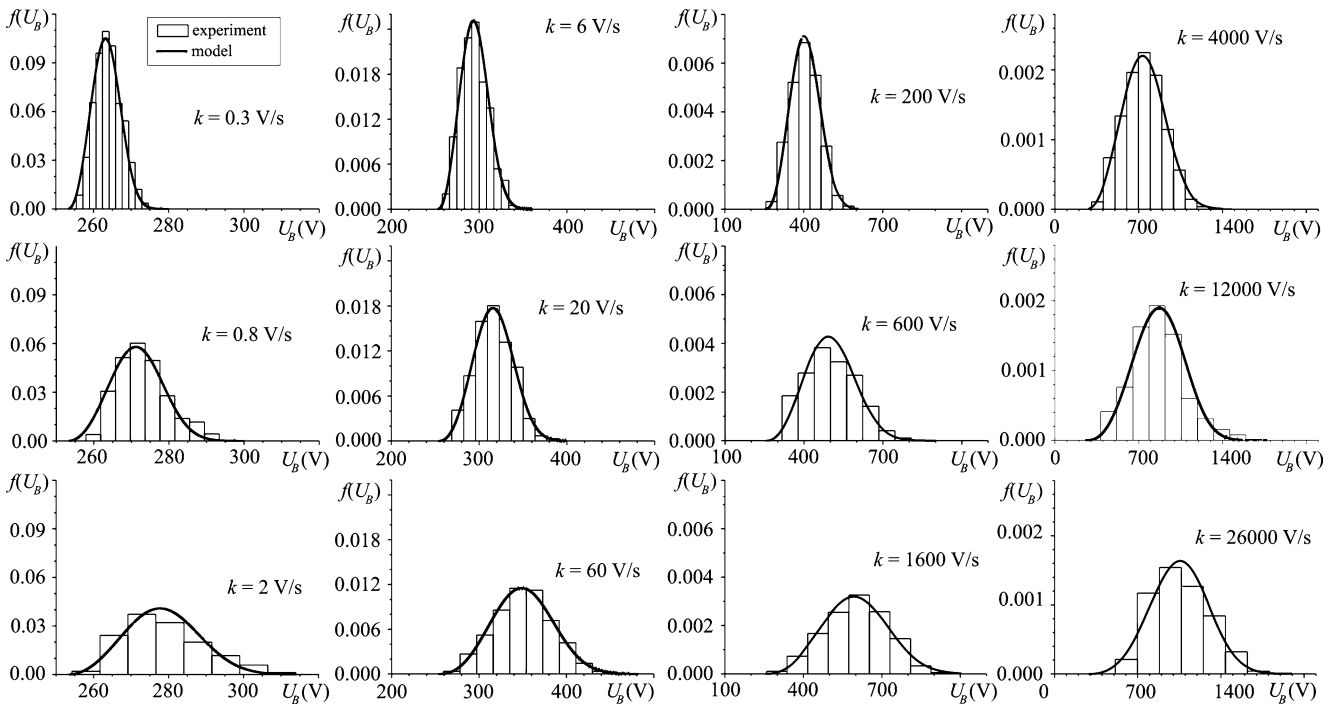

Fig. 4 Experimental (*histograms*) and theoretical (*solid lines*) breakdown voltage distributions for the indicated ramp rates k

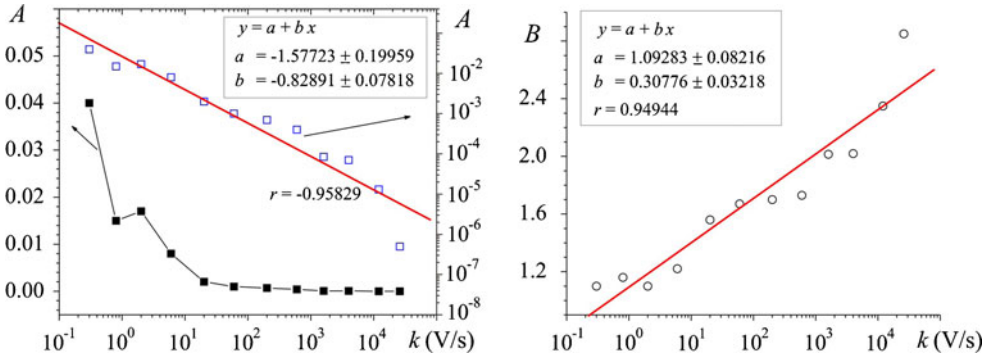

Fig. 5 (Colored online) Coefficients A and B in Eq. (7), numerically computed on the basis of the model in Section 2, as functions of the rate k. **a** Coefficient A in linear (*filled squares*) and log (*open squares*, *blue* online) scales. The *straight line* (*red* online) shows the boxed linear regression to the *open squares*. The correlation coefficient r is indicated next to the line. The *line across the filled squares* is a guide to the eye. **b** Coefficient B (*open circles*) The *straight line* (*red* online) is the boxed linear regression to the data points

side of Eq. (8), which in contrast with the prefactor A is weakly rate-dependent.

Figure 6 plots the yield Y resultant from the substitution of these values for Y_0, A, and B on the right-hand side of Eq. (8) as a function of the rate k, in logarithmic scales. The straight line displays the result of linear regression applied to the filled squares representing the computed yields. The fairly good fit implies a power law of the form $Y = a'k^b$, where $a' = \log_{10} a$, and a and b are indicated in the box at the top-left corner of the figure. This power law can alternatively be obtained from Eq. (8) and the linearity of the plots in Fig. 3. The latter implies that $U_B - U_S = \alpha\sqrt{k}$, where α is a constant. Substitution of this result the right-hand side of Eq. (8) then shows that $Y = Y_0 + A\alpha^B k^{B/2}$,

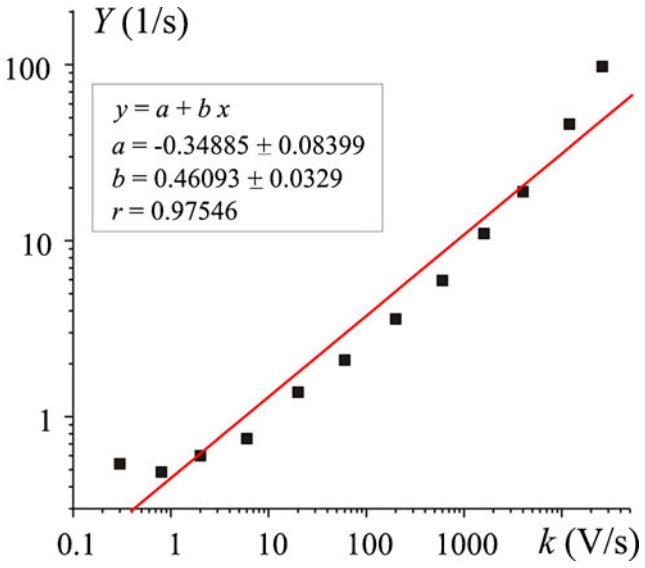

Fig. 6 (Colored online) Numerically computed yield Y as a function of k. The yield was obtained from Eq. (8), a central component of the theoretical model introduced in Section 2. The *solid line* (*red* online) represents the linear regression defined by the coefficients in the box near the *top-left corner*

and it can once again be seen that the yield is a power law of the rate k. Figure 5b shows that the exponent B varies between 1.2 and 2.4 as the rate grows, and hence that $B/2$ varies between 0.6 and 1.2, in crude agreement with the result $b = 0.46$ in Fig. 6.

The voltage dependence in Eq. (8) is due to the corona, which appears near the anode, creates free electrons, and hence raises the yield over the rest of the gap, including the region near the cathode. The enhanced yield reduces the statistical time delay, since it raises the probability of breakdown at short times. The statistical and formative time delays then become comparable, which adds a left tail to the breakdown probability distribution. Since the yield is higher at high rates, the left tail becomes more prominent at large k, while the density distribution approaches a Gaussian. The good agreement between the theoretical density distributions extracted from the proposed model and the experimental data, i. e., the good agreement between the solid lines and the histograms in Fig. 4, attest to the validity of the model.

6 Conclusion

We report experimental and theoretical results for the probability of electrical breakdown in a diode filled with Ne at 1.33 mbar. In the pre-breakdown regime, a well-defined corona is observed at the unpolished wire serving as anode. Breakdown probability distributions measured for voltages that ramp up at various rates k, varying from $k = 0.3$ V/s to $k = 26$ kV/s, are compared with our theoretical predictions.

The theoretical analysis is based on a model to which we were led by an experimental clue: the corona discharges observed in the pre-breakdown stage of our measurements. The corona is a consequence of pre-breakdown electron multiplication, a mechanism dependent on the electrode geometry. To account for pre-breakdown multiplication, our

model lets the electron yield at the cathode be a nonlinear function of the overvoltage. The theoretical expression for the breakdown voltage distribution resulting from this assumption agrees well with the experimental histograms. We conclude that our model captures adequately the physics of electrical breakdown following corona discharges.

Acknowledgments This work was supported by the Ministry of Education and Science of the Republic of Serbia (Projects III 43011 and III 43011).

References

1. J.M. Meek, J.D. Craggs. *Electrical Breakdown of Gases* (Wiley, New York, 1978)
2. M. Kristiansen, A.H. Guenther, in *Electrical Breakdown and Discharges in Gases*, ed. by E.E. Kunhart, L.H. Luessen. (Plenum, New York, 1983)
3. B. Lončar, P. Osmokrovič, S. Stankovič, IEEE Trans. Nucl. Sci. **76**, 1725 (2003)
4. M.M. Gutorov, *Basics of Light Techniques and Light Sources* (in Russian) (Moscow, Energoatomizdat, 1983)
5. K. Zuber, Annu. Phys. **76**, 231 (1925)
6. M. von Laue, Annu. Phys. **76**, 261 (1925)
7. L.B. Loeb, Rev. Mod. Phys. **20**, 151 (1948)
8. R.A. Wijsman, Phys. Rev. **75**, 833 (1949)
9. F. Llewellyn-Jones, in *Electrical Breakdown and Discharges in Gases*, ed. by E.E. Kunhart, L.H. Luessen. (Plenum, New York, 1983)
10. M. Zambra, M. Favre, J. Moreno, H. Chuaqui, E. Wyndham, P. Choi, IEEE Trans. Plasma Sci. **27**, 746 (1999)
11. J. Moreno, M. Zambra, M. Favre, IEEE Trans. Plasma Sci. **30**, 417 (2002)
12. R.S. Moss, J.G. Eden, M.J. Kushner, J. Phys. D Appl. Phys. **37**, 2502 (2004)
13. E. Wagenaars, M.D. Bowden, G.M.W. Kroesen, Plasma Sources. Sci. Technol. **14**, 342 (2005)
14. M.K. Radović, Č.A. Maluckov, S.A. Rančev, IEEE Trans. Plasma Sci. **35**, 1738 (2007)
15. M. Radović, M. Pejović, D.A. Bošan, in *Contrib. Papers of the 13th Int. Symp. on the Phys. on Ionized Gases, Sibenik*, ed. by M.V. Kurepa. (Univ. Belgrade, Belgrade, Yugoslavia, 1986), pp. 439–442
16. M.M. Pejović, R.D. Filipović, Int. J. Electron. **20**, 251 (1989)
17. M. Radović, T. Jovanović, Č. Maluckov, O. Stepanović, Balkan Phys. Lett. **5**, 1447 (1997)
18. M. Pejović, G.S. Ristić, J.P. Karamarković, Phys. J. D Appl. Phys. **35**, 91 (2002)
19. M. Radović, Č. Maluckov, IEEE Trans. Plasma Sci. **29**, 832 (2001)
20. Č.A. Maluckov, M.K. Radović, Contrib. Plasma Physics. **42**, 556 (2002)
21. Č.A. Maluckov, M.K. Radović, IEEE Trans. Plasma Sci. **30**, 1579 (2002)
22. S.D. Mitić, Č.A. Maluckov, M.K. Radović, Contrib. Plasma Physics. **46**, 292 (2006)
23. M.K. Radović, Č.A. Maluckov, M.K. Radović, IEEE Trans. on Plasma Sci. **35**, 1738 (2007)
24. Y.P. Raizer, in *Mathematical Statistics with Applications*. *Gas Discharge Physics, Springer-Verlag, Berlin Heidelberg, Germany, 1991.* (Belmont, Duxbury, MA, 1996), pp. 663–668